A Hydrophobic Patchwise Heterogeneous Oxide Surface

Leonardo Formaro,* Roberto Giannantonio, Cristina Pastorelli, and Riccardo Carli

Department of Physical Chemistry and Electrochemistry, University of Milan, Via Golgi 19, 20133 Milan, Italy
(Received: January 27, 1992)

The interfacial behavior of two CoOOH samples in aqueous solutions is investigated by means of acid–base titrations. One of the samples is characterized by unusually low values of surface charge and capacitance, in accordance with the behavior of a hydrophobic surface. Analysis of the results further shows the presence of surface regions (patches) which adsorb protons independently. These singularities are supported by ex situ XPS determinations and evidenced by the comparison with the auxiliary CoOOH companion sample.

Introduction

Oxides have anisotropic crystallographic structures[1] and can frequently accept variations from nominal compositions.[2] Unless special methods of preparation are used, they are also polycrystalline. Oxides surfaces can therefore generally be seen as aggregates of several elementary surfaces with individual extension, orientation, atomic arrangement, and composition.[3] Several examples exist of oxide–gas systems where certain surface orientations can give rise to a specific adsorption affinity or reactivity toward contacting molecules (e.g. ref 4 and references therein). For oxide–solution interfaces recent papers have shown that surfaces with different orientations should have specific structure-dependent ion-adsorption properties[5,6] and should be characterized by various kinds and degrees of heterogeneity.[7-10] Here we contribute to the subject by reporting in a preliminary form the peculiar differences between two samples of CoOOH prepared from powders of the same compound (β-$Co(OH)_2$) precipitated from aqueous solutions as highly crystalline particles with, however, different size and shape. The differences concern both qualitative and quantitative aspects of the H^+/OH^- adsorption isotherms (σ_0(pH) curves), the wettability of the powders, and the composition of the surfaces as determined by ESCA analyses.

Experimental Section

Materials. Chemicals of reagent grade quality (Baker) and water from a Milli-Q apparatus (Millipore) were used.

The investigated samples are denoted p-CoOOH, for prismatic, and s-CoOOH, for shapeless, by reference to the morphology of the particles of the precursor β-$Co(OH)_2$ (p- and s-$Co(OH)_2$). The hydroxides were precipitated by dropwise adding 2.2×10^{-2} M KOH (for s-$Co(OH)_2$) or ammonia (for p-$Co(OH)_2$) to 1×10^{-2} M $Co(NO_3)_2$ solutions preheated at 343 K. Other reaction conditions were N_2 purging before and during the reaction, and 0.5 h heating. Both precipitates were extensively washed, filtered, dried, and stored in a N_2-purged desiccator. p-$Co(OH)_2$ is formed by particles having the shape of very regular thin, hexagonal prisms, 1–2 μm wide and $\cong$0.05 μm thick, predominantly exposing the basal planes. A detailed report of the reaction will be given elsewhere.[11] s-$Co(OH)_2$ instead shows particles 0.1–0.2 μm wide, without any detectable shape regularity.

The CoOOH samples were obtained by thermal oxidation of the hydroxides ($4Co(OH)_2 + O_2 \rightarrow 4CoOOH + 2H_2O$) in a slowly rotating glass tube continuously flushed by pure O_2 (20 L/h) and heated (433 K) in a controlled temperature oven.

As shown by the values of specific surface area (BET, N_2) the oxidation causes particle fragmentation, more extensive for p- than for s-$Co(OH)_2$ (p-$Co(OH)_2$ = 4.2, p-CoOOH = 46.4, s-$Co(OH)_2$ = 24.8, s-CoOOH = 46.3 m^2/g). Nevertheless, the particles of p-CoOOH retain the overall prismatic shape of the parent hydroxide.

The phase composition of all the samples was carefully controlled by X-ray diffraction (XRD). No contaminants were detected.

Interfacial Determinations. Aqueous suspensions of the samples were investigated using the well-documented acid–base "fast titration" technique.[12] Before measurements, powders were equilibrated overnight at the spontaneous pH in the presence of the lowest base electrolyte concentration (1×10^{-3} M KNO_3). pH was measured to 1×10^{-3} unit resolution using separate glass and calomel electrodes. Titrants (0.1 M HNO_3 and KOH) were added only when the time variation of pH became slower than 0.003 pH/min. The criterion was met in 5–8 min after each addition. The first titration was discarded. Hysteresis between any two successive acid and base titrations at the same electrolyte concentration was generally lower than 0.2 μequiv/cm^2.

To verify the absence of long-term irreversible processes, at the end of the first titration cycle, the oxides were recovered from the suspensions, centrifuged, redispersed in N_2-degassed water, stored for 20 days in water, and titrated once more. The two sets of titrations superimposed on each other within a very narrow tolerance. The adsorbed amounts of H^+/OH^- are reported vs pH as the surface charge, σ_0 normalized with respect to the BET surface areas.

XPS Measurements. X-ray photoelectron spectra were taken in a Surface Science Instruments M-Probe ESCA with base pressure of 1.0×10^{-9} Torr. The equipment features a high-vacuum reaction chamber allowing for thermal treatments in a controlled atmosphere.[13] A monochromated Al Kα radiation source was used. Survey and single-element analyses were obtained using a spot size of 400×1000 μm^2 (pass energy 150 eV) and 200×750 μm^2 (pass energy 25 eV), respectively. Samples were pressed onto an insulating biadhesive tape and outgassed for 12 h at the operating pressure. Because of their insulating nature, a flood gun was used for complete charge neutralization.[14] The (1s) level of adventitious carbon (atmospheric hydrocarbons and surface carbon oxides) is taken as the internal standard with

(1) Wells, A. F. *Structural Inorganic Chemistry*; Oxford University Press: London, 1962.
(2) Kröger, F. A. *The chemistry of Imperfect Crystals*; North Holland Publishing Company: Amsterdam, 1964.
(3) Henrich, V. E. *Prog. Surf. Sci.* **1983**, *14*, 185.
(4) Bolis, V.; Fubini, B.; Giamello, E. *J. Chem. Soc., Faraday Trans. 1* **1989**, *85*, 105.
(5) Hiemstra, T.; van Riemsdijk, W. H.; Bolt, G. H. *J. Colloid Interface Sci.* **1989**, *133*, 91.
(6) Hiemstra, T.; De Witt, J. C. M.; van Riemsdijk, W. H. *J. Colloid Interface Sci.* **1989**, *133*, 105.
(7) van Riemsdijk, W. H.; Koopal, L. K.; De Witt, J. C. M. *Netherlands J. Agric. Sci.* **1987**, *35*, 241.
(8) van Riemsdijk, W. H.; De Witt, J. C. M.; Koopal, L. K.; Bolt, G. H. *J. Colloid Interface Sci.* **1987**, *116*, 511.
(9) Koopal, L. K.; van Riemsdijk, W. H. *J. Colloid Interface Sci.* **1989**, *128*, 188.
(10) Gibb, A. W. M.; Koopal, L. K. *J. Colloid Interface Sci.* **1990**, *134*, 122.
(11) Barberis, L.; Formaro, L.; Millini, G. Manuscript in preparation.
(12) Breeuwsma, A.; Lyklema, J. *Discuss. Faraday Soc.* **1971**, *52*, 324.
(13) Bianchi, C.; Cattania, M. G.; Ragaini, V. *Mater. Chem. Phys.* **1991**, *29*, 297.
(14) Bryson, C. E., III *Surf. Sci.* **1987**, *189/190*, 50.

0022-3654/92/2096-3197$03.00/0

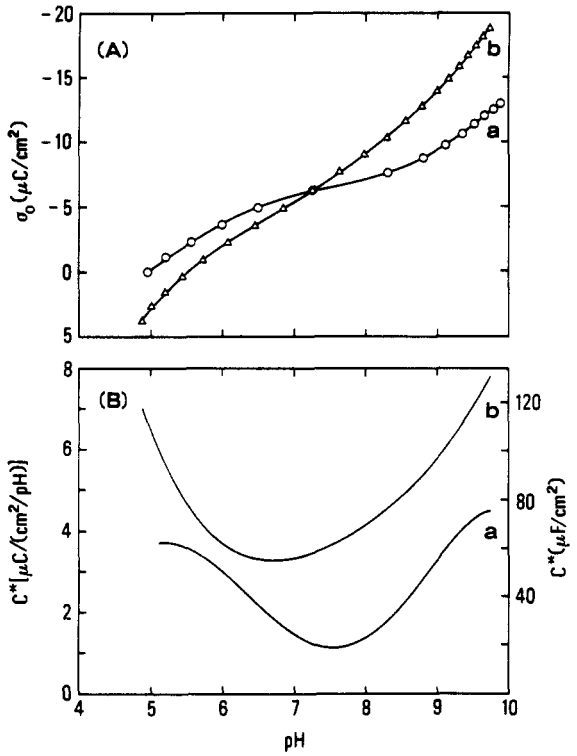

Figure 1. (A) σ_0(pH) curves of s-CoOOH in (a) 1×10^{-3} M, (b) 0.1 M KNO_3. Relative σ_0 values (see text). (B) Operational differential capacitances of s-CoOOH from numerical elaboration of data in Figure 1A.

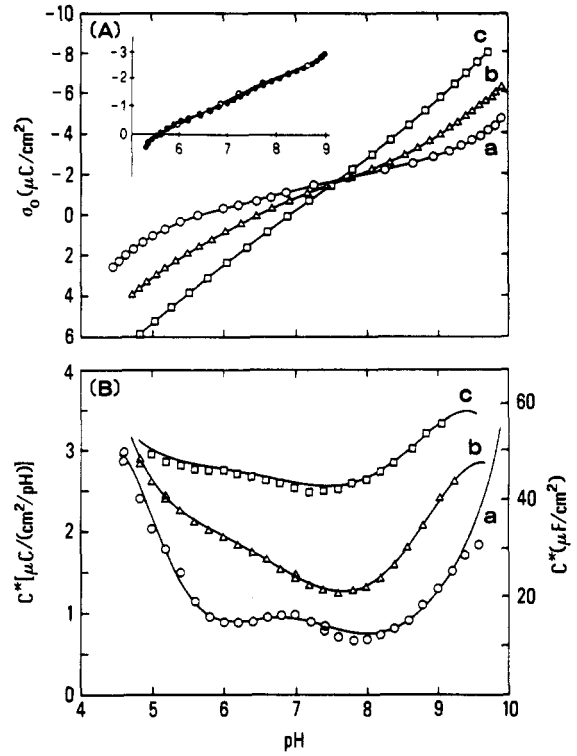

Figure 2. (A) σ_0(pH) curves of p-CoOOH in (a) 1×10^{-3} M, (b) 0.01 M, (c) 0.1 M KNO_3. Relative σ_0 values (see text). (B) Operational differential capacitances from numerical (lines) and graphical (points) elaboration of data in Figure 2A.

peak position at 284.6 eV. Numerical and graphical elaborations of the spectra were performed by The Surface Science Instruments software.

Discussion

Figures 1A and 2A show the σ_0(pH) curves from acid base titrations of s- and p-CoOOH, respectively. The differentials of the plots, $(\partial\sigma_0/\partial pH)_I = C^*$, are reported vs pH in Figures 1B and 2B. C^* is the operational differential capacitance at a given ionic strength, I, recently reintroduced[9,10] as it can afford a detailed insight on the interfacial behavior of oxides. Differentiation was performed both graphically and by cross-checking the results of standard numerical routines (cubic spline interpolation and least-squares polynomial fitting followed by differentiation of the resulting functions[15]).

s-CoOOH closely fits the familiar behavior of many amphoteric oxides. The crossover point of the curves in Figure 1A does not coincide with the inflection points of either of them, and further, with increasing the KNO_3 concentration, the inflection points shift to more positive σ_0 values. These features indicate that K^+ specifically interacts with the surface, thus preventing the zero charge condition ($\sigma_0 = 0$; pzc) of the surface from being specified.[16,17] From the C^*(pH) curves (Figure 1B), the specific interactions are seen to be concentration dependent. In 1×10^{-3} M KNO_3 a deep minimum (pH $\cong$ 7.7) is present between rapidly increasing capacitance branches. For pH $\cong$ 5.5–9.2 the curve is highly symmetrical around the minimum, thus suggesting that any pH variation causes equal and opposite incremental charges to accumulate on the surface. The same condition also holds for the compensating counter charge in solution. The symmetry of the curve therefore shows that at the relevant electrolyte concentration, K^+ and NO_3^- interact with the surface with no or only small excess energies in respect to each other. Prevailing Coulombic nonspecific interactions between the electrolyte and a pristine surface[16-18] are hence indicated. In 0.1 M KNO_3 the curve is displaced to larger C^* values and, what is most relevant, it shifts to the left of the previous one with a skewed symmetry. As a whole, this shows that at the considered electrolyte concentration the compensation of the H^+/OH^- surface charge more efficiently occurs when the surface is negative and the counterion positive than contrariwise. Specific interactions between the surface and K^+ occur, as induced by the increased electrolyte concentration.

The capacitance results conform to the behavior of either a homogeneous or a random heterogeneous surface.[9] The electrical equivalent of these surfaces contains a basic (Stern) inner layer and a diffuse layer capacitor connected in series. In a symmetrical background electrolyte, only one minimum occurs at a distance from the pzc which depends on whether and to what extent specific interactions develop.

The σ_0(pH) curves of p-CoOOH do not show a precise crossover point (Figure 2A), preventing also in this case the zero charge condition of the sample from being specified.[16,17] By analogy with the behavior of s-CoOOH this might arise from specific surface electrolyte interactions. Entirely different reasons however intervene, related to the particular shape of the curve in 1×10^{-3}M KNO_3. Two concavities to the pH axis are in fact present, one of them appearing just at intermediate σ_0 and pH, i.e., exactly where intersections with the curves at higher electrolyte concentrations should occur. For the sake of clarity and to show the reproducibility of the result, the inset to Figure 2A compares two independent experiments with different oxide amounts in a given solution volume (for other reproducibility tests, see the Experimental Section). The curve is quite unusual. For comparable electrolyte concentrations all of the results we are aware of show only weak and almost linear charge variations around a single inflection point.

When KNO_3 is added, the additional concavity disappears, and the curves become steeper and almost featureless.

Meaningful additional details emerge from the C^*(pH) data in Figure 2B. In the most dilute solution two minima are clearly seen at pH $\cong$ 6 and 8. Assuming that the surface potential, ψ_0,

(15) Press, W. H.; Flannery, B. P.; Teukolsky, S. A.; Vetterline, W. T. *Numerical Recipes*; Cambridge University Press: Cambridge, 1990.
(16) Lyklema, J. *J. Colloid Interface Sci.* **1984**, *99*, 109.
(17) Ardizzone, S.; Formaro, L.; Lyklema, J. *J. Electroanal. Chem.* **1982**, *133*, 147.
(18) Pyman, M. A. F.; Bowden, J. W.; Posner, A. M. *Austr. J. Soil Res.* **1979**, *17*, 191.

obeys a Nernstian pH dependence the minima are found at extraordinarily low capacitance values, $C^* \cong 15$ and 11 $\mu F/cm^2$ (see the auxiliary axis). At higher concentrations the curves are anyhow asymmetric along the pH axis, and on the left they show nearly pH-independent regions with a well-defined minimum at pH $\cong$ 7.7.

The morphology of the curves does not agree in any simple way with the behavior of random heterogeneous or homogeneous surfaces. It is here proposed that the surface is heterogeneous with (at least) two independent regions which individually behave homogeneously and respond to variations in the activity of H^+/OH^- and of the electrolyte. In the terminology used by Koopal et al.,[9] the surface is patchwise heterogeneous with noninteracting (homogeneous) patches. The overall capacitance of the surface additively results from two capacitances connected in parallel, each representing one patch and comprising a diffuse and a Stern layer capacitor. The separate minima in curve a are of primary concern. They resemble the near parabolic shape of total capacitance vs potential, $C_T(E)$, relationships calculated by double layer theory[19,20] for low rational potentials and ionic strength. Rather special conditions have however to take place so that the minima of two independent $C_T(E)$ curves can still appear in their parallel $C_{T,p}(E)$ superposition. At some potential distance from both pzc's, the larger capacitance of the one patch should in fact tend to mask the minimum of the other. Accordingly, for comparable low electrolyte concentrations no similar evidence could be found regarding oxides or patchwise single crystal metal electrodes.

Exploratory calculations were performed assuming that the patches have equal surface areas and surface potentials obeying a Nernstian pH dependence from different pzc values. The basic Stern–Gouy–Chapman (SGC) model was used as outlined in ref 20. So far the results present discordant aspects. $C_{T,p}(\psi_0)$ (or $C_{T,p}$(pH)) plots readily show two minima with $C_T \cong 11$ $\mu F/cm^2$ separated by ψ_0 (or pH) distances which correspond with the experimental values ($\Delta\psi_0 \cong 120$ mV or 2 pH units) only if very low and comparable Stern capacitances are used, e.g., 23–26 $\mu F/cm^2$. If, however, somewhat larger and more divergent C_{Stern} values are used, the minima tend to merge together, thus rendering impossible to reproduce the separation of the minima *and* their absolute value. The lack of quantitative agreement with experimental data is more probably due to some limitation of the used assumptions than to an inadequacy of the qualitative picture of the interface. This is in fact further supported by the effects introduced by variations of electrolyte concentration. In 0.01 M KNO_3 (curve b) only one deep minimum is present followed by a slowly rising capacitance region at lower pH values. By comparison with curve a this shows that the patches are differently influenced by the electrolyte concentration, and therefore, still relying on the SGC model, they have somewhat different Stern capacitances, the larger one being associated with the patch characterized by the deep minimum. In this connection, no distinction can be made between specific (per unit area) and total capacitances, the relative surfaces of the patches being in fact unknown. In 0.1 M KNO_3 the patch with the larger Stern capacitance still appears through the wide shallow minimum on the right of the curve. The pH-independent region on the left also in this case suggests a secondary patch with a lower Stern capacitance, almost saturated at the relevant electrolyte concentration.

The samples differ from each other also quantitatively. In the pH range 5–9.5 the variation of σ_0 of p-CoOOH amounts to 4.6 and 12.6 $\mu C/cm^2$ in 1×10^{-3} and 0.1 M KNO_3, respectively. These values compare with 11.0 and 20.0 $\mu C/cm^2$ for s-CoOOH (see Figures 1A and 2A). As σ_0 is in any case normalized on the BET surface area of the samples, the results from BET and H^+/OH^- adsorption give an apparently different estimate of the available surface areas. Considering, however, that H^+/OH^- adsorption takes place at discrete surface sites, these results show that the samples definitely differ for the density of H^+-adsorbing surface sites, with a relative value of p-CoOOH/s-CoOOH $\cong$ 0.63 (from the data in 0.1 M KNO_3).

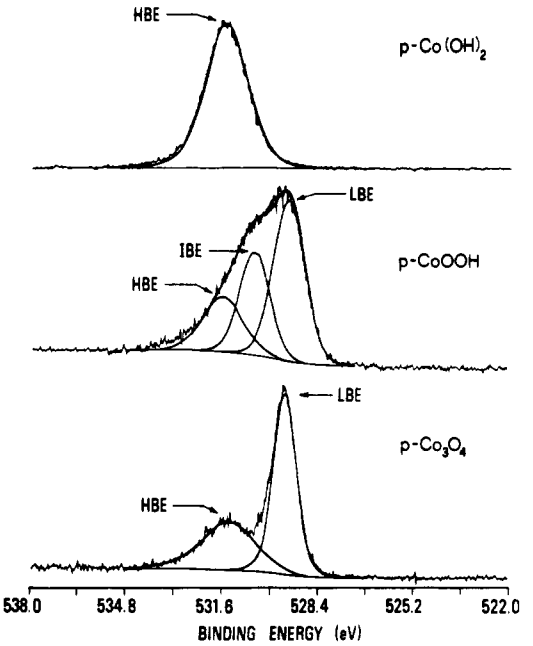

Figure 3. XPS spectra of the indicated samples in the O(1s) region.

TABLE I: Binding Energies and Relative Abundance of the Deconvoluted O(1s) Peak Components of the s- and p-CoOOH Samples

	s-CoOOH	p-CoOOH
LBE, eV	529.5	529.4
IBE, eV	530.5	530.5
HBE, eV	531.6	531.6
RHL (HBE/LBE)	0.82	0.43
RIL (IBE/LBE)	0.68	0.60

Similar differences also exist between the C_{Stern} values of the samples. Far from the pzc and at high electrolyte concentrations total capacitances are dominated by Stern layer values. The capacitance value where C^*(pH) curves tend to flatten gives an approximate estimate of C_{Stern}. For p-CoOOH (Figure 2B) this value is not far from 60 $\mu F/cm^2$. No similar tendency appears in Figure 1B, hence showing that C_{Stern} of s-CoOOH has a larger value, perhaps in the range 100–200 $\mu F/cm^2$. From this respect, p-CoOOH more closely resembles the behavior of hydrophobic interfaces as AgI or Hg,[21,22] characterized by rather low Stern capacitances ($\cong$30 $\mu F/cm^2$). It can further be mentioned that the macroscopic behavior of the suspensions also agrees with different hydrophobic properties of the samples: the particles of p-CoOOH tend to float at the free surface of solutions and to creep upward in vertical meniscuses. No similar effect was instead observed for s-CoOOH.

An independent assessment of the properties of the surfaces was sought by means of XPS determinations.

Elemental analyses of either oxide did not reveal any trace of impurity, the only surface species identified being Co, O, C.

Results on the O(1s) region are especially relevant to the kind and number of surface oxygen species (O^{2-}, OH, O^-, H_2O). Figure 3 shows the experimental O(1s) peak of one of the samples. In agreement with literature data,[23-26] a low and a high binding energy component (LBE and HBE, respectively) are present (see

(19) Barlow, C. A., Jr. *Physical Chemistry*; Eyring, H., Ed.; Academic Press: New York, 1970; Vol. IXA, Chapter 2.
(20) Hunter, R. J. *Foundations of Colloid Science*; Clarendon Press: Oxford, 1986; Vol. I, Chapter 6.
(21) Trasatti, S. *Croat. Chem. Acta* **1987**, *60*, 357.
(22) Fokkink, L. G. J.; De Kaizer, A.; Lyklema, J. *J. Colloid Interface Sci.* **1989**, *127*, 116.
(23) Chuang, T. J.; Brundle, C. R.; Rice, D. W. *Surf. Sci.* **1976**, *59*, 413.
(24) McIntyre, N. S.; Cook, M. G. *Anal. Chem.* **1975**, *47*, 220.
(25) Gonzales-Elipe, A. R.; Espinos, J. P.; Fernandez, A.; Munuera, G. *Appl. Surf. Sci.* **1990**, *45*, 103.
(26) Tyuliev, G.; Angelov, S. *Appl. Surface Sci.* **1988**, *32*, 381.

also Table I). A third non-previously-reported component is also present at intermediate binding energy (IBE). The attribution of the peak components was investigated in greater detail recording the spectra of $Co(OH)_2$ and Co_3O_4 (both s- and p-modifications). These latter oxides were prepared by heating in O_2 s- and p-$Co(OH)_2$ in the XPS reaction chamber at 573 K; their spinel structure was confirmed by XRD.

The hydroxides consistently showed a single peak near 531.4 eV, with a broadness related to the neighborhood-dependent differential charging of surface hydroxyl groups.[15,27] The spinels had a characteristic peak at 529.1 eV with a sharpness (fwhm $\cong$ 0.9 eV) related to O^{2-} lattice ions in highly crystalline Co_3O_4. The principal deconvoluted components of the CoOOH's O(1s) peak are therefore assigned to hydroxyl species and lattice oxygen, respectively. No additional evidence was obtained for the IBE component. By analogy with other results,[28] the peak is tentatively attributed to strongly chemisorbed water, remaining at the surface after the hydroxide decomposition.

A small fraction of the total surface cobalt is present as Co^{2+}. This was verified by weighing the multiplet splitting doublet component of the Co(3s) photoelectron peak.[29,30] The Co^{3+}/Co^{2+} ratio has quite similar values in both s- and p-CoOOH, so that any influence of a different distribution of the metal ion oxidation state on the surface oxygen polarization can be safely neglected.

The relative abundances of HBE and IBE species with respect to lattice oxygen, LBE (chosen as the internal reference), were therefore estimated from the ratio of the deconvoluted peak areas, RHL = HBE/LBE and RIL = IBE/LBE (see Table I). It has to be noted that RHL, RIL, and Co^{3+}/Co^{2+} cannot be influenced by kinetic energy (E) dependent factors since the relevant chemical species have very close kinetic energies (ΔE = 1.0–2.0 eV). In particular, a damping factor due to contaminating carbon overlayers can be excluded.[31]

Notably enough, the abundance of OH groups has different values for the samples, with a relative value ($RHL_{p\text{-}CoOOH}/RHL_{s\text{-}CoOOH} \cong 0.52$) rather close to the (relative) density of H^+-adsorbing surface groups previously indicated on σ_0(pH) results. A better agreement could be obtained depending on the nature of the IBE component, which is currently under investigation.

Conclusions

The transformation of β-$Co(OH)_2$ to CoOOH occurs with an increase of specific density[32] and involves compounds with essentially the same layer structure.[1] We believe that the properties of the samples are due to a different manner the crystals of the original $Co(OH)_2$ powders collapse under the anisotropic strains which occur during the thermal oxidation and hence expose surfaces with prevailing different structure and orientation, OH site occupancy, and charge acquisition capability. For p-CoOOH the density of OH groups is apparently so low as to induce a hydrophobic behavior and to allow energetically different site ensembles to appear within the general amphoteric response of the overall surface.

Acknowledgment. Financial support from the Ministry of University, Scientific and Technological Research (MURST) and in part from Eniricerche SpA (Milano) is gratefully acknowledged.

(27) Jaegle, A.; Kalt, A.; Nanse, G.; Perucchetti, J. C. *J. Electron Spectrosc. Relat. Phenom.* **1978**, *13*, 175.
(28) Clarke, N. S.; Hall, P. G. *Langmuir* **1991**, *7*, 672.
(29) Frost, D. C.; Mc Dowell, C. A.; Woolsey, I. S. *Chem. Phys. Lett.* **1972**, *17*, 320.
(30) Briggs, D.; Gibson, V. A. *Chem. Phys. Lett.* **1974**, *25*, 493.
(31) Defossé, C. *Characterization of Heterogeneous Catalysts*; Delannay, F., Ed.; Marcel Dekker: New York, 1984; Chapter 6.
(32) *Handbook of Chemistry and Physics*, 51st ed.; Weast, R. C., Ed.; The Chemical Rubber Co.: Cleveland, 1970.